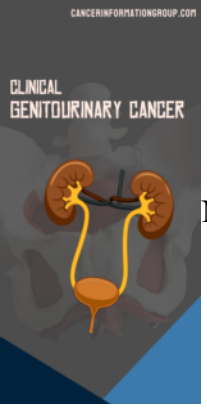

CLINICAL GENITOURINARY CANCER,
ISSN / eISSN 1558-7673 / 1938-0682
Publisher CIG MEDIA GROUP, LP,
3500 MAPLE AVENUE, STE 750, DALLAS,
USA, TX, 75219-3931
Volume 26-Issue 1-(2026)
DOI:http://doi.org/10.65613/737127

OPEN ACCESS

NDRG1 in uterine corpus endometrial carcinoma: prognostic significance and associations with TP53 context and ferroptosis-related transcriptional programs

Check for updates

Yumei Yang[1], Yi Zhao[1], Yifan Qin[2], Bayasalahu[1], Huixin Chen[2], Jianying Mao[3]*

[1] Inner Mongolia Medical University, Hohhot, Inner Mongolia, China

[2] Baotou Medical College, Inner Mongolia University of Science and Technology, Baotou, Inner Mongolia, China

[3] Inner Mongolia Autonomous Region People's Hospital, Hohhot, Inner Mongolia, China

* Corresponding author: Jianying Mao; Email: 13684742432@qq.com

Abstract

Background: Uterine corpus endometrial carcinoma (UCEC) is molecularly heterogeneous, and clinically relevant biomarkers that link tumor biology to outcome remain needed. N-myc downstream-regulated gene 1 (NDRG1) is a stress-responsive gene with context-dependent roles in cancer and plausible connections to TP53-associated ferroptosis, but its significance in UCEC has not been systematically defined.

Methods: Public TCGA-UCEC transcriptomic and clinical data were obtained from publicly accessible TCGA/GDC-derived resources. We evaluated NDRG1 expression, clinicopathological and survival associations, TP53 context, ferroptosis-related signatures, and pathway enrichment, and performed exploratory progression-free interval (PFI) modeling.

Results: NDRG1 was downregulated in UCEC tumors relative to normal endometrium; however, within tumors, higher NDRG1 expression identified a clinically aggressive subset characterized by worse overall survival, disease-specific survival, and PFI, together with enrichment of higher grade, advanced stage, and non-endometrioid histology. NDRG1 was further linked to a TP53-contextual biological state: expression tended to be higher in TP53-mutant tumors, ferroptosis activity differed significantly by TP53 status and TP53×NDRG1 subgroup, and GSEA showed enrichment of a p53 downstream pathway in NDRG1-high tumors. In the normalized cohort, NDRG1 correlated positively with ATG5, TFRC, FTH1, and VTCN1 and negatively with CTLA4, supporting an association with ferroptosis-related and immunoregulatory transcriptional programs.

Conclusions: NDRG1 identifies an adverse UCEC subset and resides within a TP53-contextual, ferroptosis-related transcriptional landscape. These findings support NDRG1 as a candidate biomarker for prognostic and biological stratification in UCEC and provide a rationale for further mechanistic and translational investigation of the NDRG1-TP53-ferroptosis axis.

Keywords: NDRG1; TP53; ferroptosis; uterine corpus endometrial carcinoma; prognosis; TCGA

Introduction

Uterine corpus endometrial carcinoma (UCEC) encompasses tumors with markedly diverse biological behaviors and clinical outcomes. This heterogeneity is clinically important because corpus uteri cancer accounted for more than 420,000 new cases and nearly 98,000 deaths worldwide in 2022[1]. Although many patients present with localized disease, relapse and death

remain concentrated in biologically aggressive subtypes[2]. TCGA-based molecular classification has refined risk stratification in UCEC, but transcript-level markers that complement clinicopathological assessment remain of interest[3].

Among the processes that may contribute to this heterogeneity, ferroptosis has attracted considerable attention. Ferroptosis is an iron-dependent form of regulated cell death driven by lipid peroxidation and embedded within broader metabolic and redox networks[4-6]. It has emerged as a potential therapeutic vulnerability in cancer[7]. TP53 is especially relevant in this context because it can modulate ferroptosis through metabolic and redox pathways, although the direction and magnitude of this effect are strongly context dependent[8,9].

Against this background, N-myc downstream-regulated gene 1 (NDRG1) is of particular interest. NDRG1 is a stress-responsive gene involved in differentiation, metabolism, survival, and tumor progression[10-12]. In endometrial carcinoma, prior work has linked NDRG1/PTEN expression to adverse clinicopathological features[13]. Experimental evidence has also connected NDRG1 with p53-mediated genome-stability programs[14]. Together, these observations raise the possibility that NDRG1 may mark aggressive UCEC and intersect with TP53 context and ferroptosis-related transcriptional states.

Accordingly, we analyzed public TCGA-UCEC data to characterize the expression landscape and prognostic relevance of NDRG1, define its clinicopathological associations, explore TP53-contextual patterns, evaluate associations with ferroptosis regulators and immune checkpoint genes, and examine pathway-level enrichment. We also explored whether integrating NDRG1 with clinical and molecular covariates could improve individualized PFI estimation in a complete-case cohort.

Materials and methods

Data sources and analytical cohorts

Public TCGA-UCEC RNA-seq expression profiles and corresponding clinical annotations were obtained from publicly accessible TCGA/GDC-derived resources. Unless otherwise specified, tumor-normal comparisons, clinicopathological analyses, and primary survival analyses were based on the TCGA-UCEC tumor TPM expression matrix transformed as log2(TPM+1). Survival endpoints, including overall survival (OS), disease-specific survival (DSS), and progression-free interval (PFI), were obtained from the TCGA Pan-Cancer Clinical Data Resource (TCGA-CDR)[15].

Some figure panels were based on smaller matched cohorts rather than on the full 554-tumor TPM cohort. Selected mutation-stratified and correlation analyses used a publicly available normalized HiSeqV2 expression matrix, and sample size decreased further after TP53 mutation annotations were matched to expression sample identifiers. The exact data source, scale, and final sample size for each main figure panel are summarized in S5 Text.

Differential expression and clinicopathological analyses

NDRG1 expression was profiled across TCGA cancer projects and compared between tumor and normal tissues. For UCEC, both unpaired tumor-normal and paired tumor-adjacent comparisons were performed.

In clinicopathological subgroup analyses, normal tissues were excluded and tumors were dichotomized into NDRG1-high and NDRG1-low groups using the cohort median NDRG1 value.

Depending on the data distribution and variance structure, two-group comparisons were performed using Student's t-test, Welch's t-test, or the Wilcoxon rank-sum test. Multi-group comparisons were performed using the Kruskal-Wallis test followed, when appropriate, by Dunn's post hoc procedure. Clinicopathological contingency summaries are provided in Table 1.

Survival analyses

Kaplan-Meier curves were generated for OS, DSS, and PFI using the median NDRG1 value as the primary cutoff. Hazard ratios (HRs) and 95% confidence intervals (CIs) were estimated using univariate Cox proportional hazards regression with the NDRG1-low group as the reference.

TP53-context exploratory analyses

To examine whether NDRG1-related associations varied by TP53 context, we performed three complementary analyses. First, we assessed the correlation between NDRG1 and TP53 mRNA expression in the full TPM cohort. Second, in a matched normalized-expression cohort, we compared NDRG1 expression between TP53-wild-type and TP53-mutant tumors after sample-ID matching. Third, as a sensitivity analysis, TP53-stratified Kaplan-Meier curves were generated using extreme within-stratum quantiles of NDRG1 expression (bottom 20% versus top 20%) rather than the full median split.

For descriptive comparison of marker performance, time-dependent ROC analyses were generated for NDRG1 mRNA and TP53 mRNA at 1, 3, and 5 years in the overall UCEC cohort with available outcome data. These panels were used to illustrate relative discrimination rather than to claim clinical test performance.

Ferroptosis- and immune-related analyses

A curated ferroptosis gene panel was assembled from FerrDb[16]. In the normalized-expression cohort, Spearman correlations were calculated between NDRG1 and ferroptosis regulators/markers and between NDRG1 and a panel of immune checkpoint or immunoregulatory genes. Benjamini-Hochberg correction was applied to NDRG1-centric correlation summaries, whereas the heatmaps display correlation structure with nominal significance annotations.

A ferroptosis activity score (FerroptosisScore) was calculated using single-sample gene set variation analysis (ssGSEA/GSVA)[17] on a curated ferroptosis regulator gene set. The FerroptosisScore was then compared across TP53 subgroups and TP53×NDRG1 subgroups. Because not all expression-matrix samples had matched TP53 mutation annotations, some panels were based on the mutation-annotated subset, whereas others used the broader normalized-expression cohort.

Gene set enrichment analysis

Differential expression between NDRG1-low and NDRG1-high tumors was calculated from the public UCEC expression matrix, with logFC defined for NDRG1-low versus NDRG1-high tumors. Genes were ranked by logFC and analyzed using GSEA[18] against MSigDB canonical pathways (c2.cp.all.v2022.1.Hs.symbols.gmt). Because negative logFC corresponds to higher expression in the NDRG1-high group, negative normalized enrichment scores (NES) indicate enrichment in NDRG1-high tumors.

We report nominal P values, adjusted P values, and FDR/q values from GSEA. Pathways meeting the discovery-oriented FDR threshold were considered enriched, whereas pathways with weaker support were described as suggestive. Full ranked GSEA results are provided in S4 Table.

Exploratory prognostic model

To explore integrative risk modeling, we constructed a complete-case multivariable Cox model for PFI using the subset with non-missing age, stage group, grade group, TP53 mutation status, NDRG1 expression, and FerroptosisScore (n = 165). A nomogram based on this model was generated for internal illustration[19]. Reporting and interpretation were informed, where applicable, by TRIPOD transparency principles[20].

Calibration, time-dependent ROC, and decision curve analyses[21,22] were treated as internal diagnostic displays only and were not interpreted as evidence of external validation. For a compact effect-size summary in Fig 3D, we also reconstructed 2×2 contingency tables after collapsing clinical stage (II-IV versus I), histologic grade (G2-G3 versus G1), and histological type (mixed/serous versus endometrioid). These reconstruction details are provided in S5 Text.

Statistical analysis and AI disclosure

All statistical tests were two-sided. Unless otherwise specified, $P < 0.05$ was considered statistically significant. Correlation analyses used Spearman's rank method. Given the exploratory design and the use of multiple public-data subsets, non-significant findings were interpreted conservatively.

During manuscript preparation, an AI-assisted language tool (ChatGPT, OpenAI) was used to improve language clarity. The authors reviewed and edited the output and assume full responsibility for the final content.

Results

NDRG1 expression is reduced in UCEC but remains heterogeneous across tumors

Pan-cancer screening showed lineage-dependent differences in NDRG1 expression across TCGA tumor types. In UCEC, NDRG1 expression was significantly lower in tumors than in normal endometrium in both the unpaired comparison (tumor n = 554, normal n = 35; P = 0.0156) and the paired analysis of 23 matched tumor-adjacent normal pairs (P = 0.0082). These findings indicate that NDRG1 is dysregulated in UCEC while remaining substantially heterogeneous across tumors.

Fig 1. Pan-cancer and UCEC-specific expression analysis of NDRG1. (A) Differential expression of NDRG1 between tumor and normal tissues across multiple TCGA cancer types. (B) Unpaired comparison of NDRG1 expression between TCGA-UCEC tumor samples (n = 554) and normal endometrial tissues (n = 35). (C) Paired analysis of 23 matched tumor-adjacent normal pairs.

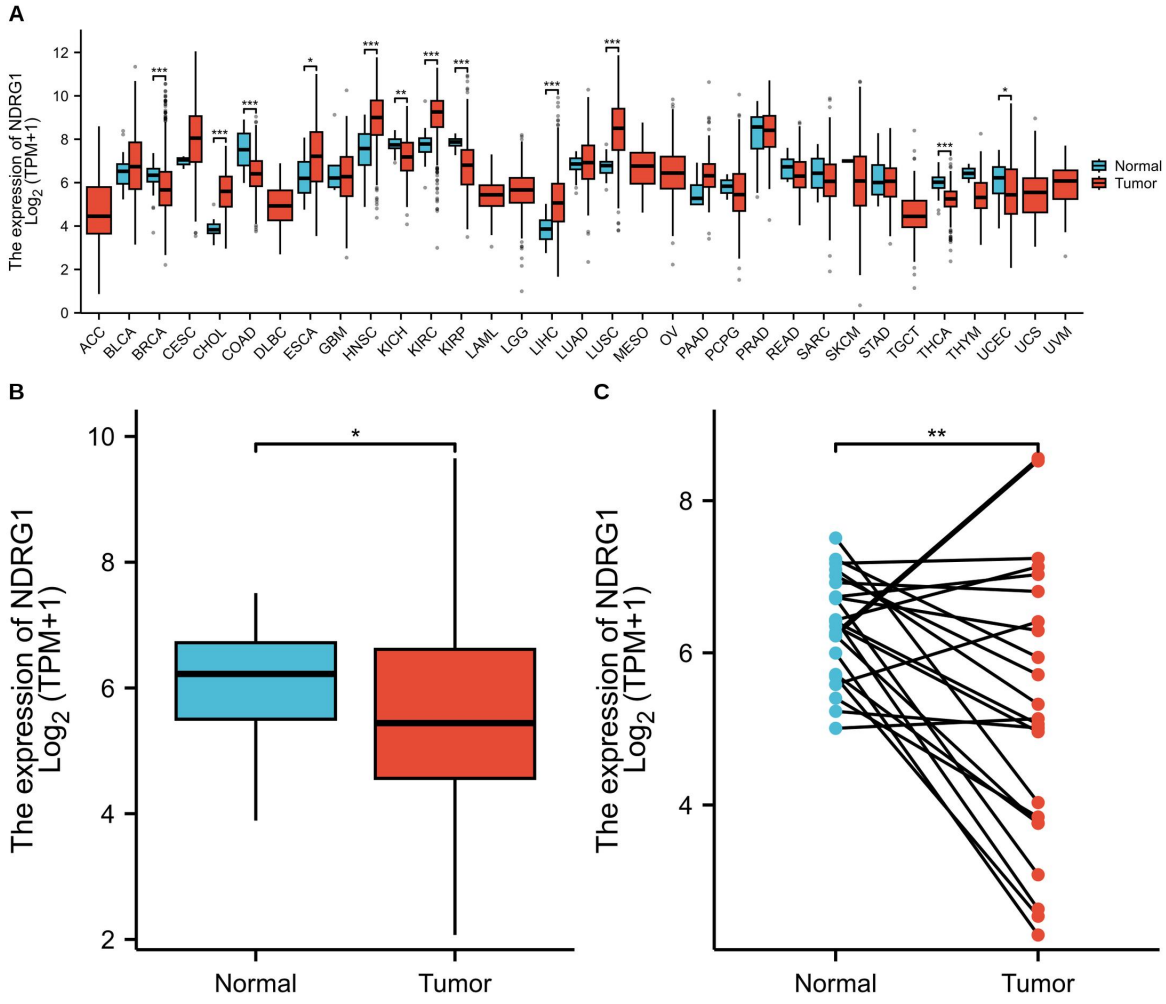

High NDRG1 expression is associated with poorer survival

Using the median NDRG1 value as the primary cutoff, Kaplan-Meier analyses showed that the NDRG1-high group had worse OS (HR = 1.79, 95% CI: 1.19-2.71, P = 0.006), PFI (HR = 1.49, 95% CI: 1.05-2.11, P = 0.025), and DSS (HR = 2.06, 95% CI: 1.23-3.45, P = 0.006) than the NDRG1-low group. The consistent direction of association across all three endpoints supports the interpretation that elevated tumor NDRG1 marks a clinically less favorable UCEC subset.

Fig 2. Prognostic associations of NDRG1 in UCEC. Kaplan-Meier survival curves for overall survival (OS), progression-free interval (PFI), and disease-specific survival (DSS) stratified by the cohort median NDRG1 expression. Hazard ratios (HRs) and 95% confidence intervals (CIs) were estimated by univariate Cox regression with the NDRG1-low group as the reference.

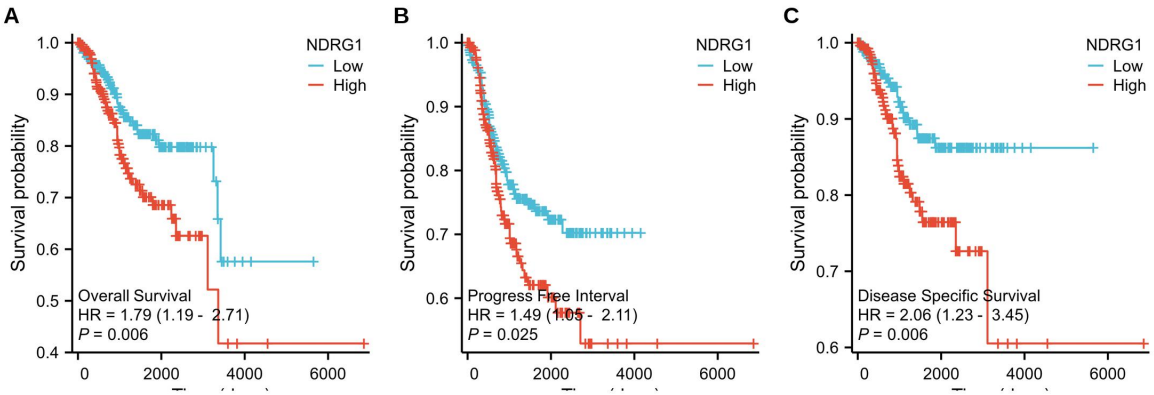

NDRG1 is associated with adverse clinicopathological characteristics

Compared with the NDRG1-low group, the NDRG1-high group contained a greater proportion of grade 3 tumors (72.6% vs 46.5%, P < 0.001) and mixed/serous histology (35.4% vs 15.9%, P < 0.001). A higher proportion of stage II-IV disease was also observed in the NDRG1-high group, although this comparison was borderline significant (32.9% vs 24.5%, P = 0.061). Expression-level subgroup analyses likewise showed higher NDRG1 values in more advanced stage groups, in grade 3 tumors, and in mixed/serous tumors than in endometrioid tumors. Reconstructed odds-ratio summaries further confirmed enrichment of high NDRG1 expression in tumors with advanced stage (OR = 1.612, 95% CI: 1.140-2.277, P = 0.007), high grade (OR = 3.644, 95% CI: 2.232-5.951, P < 0.001), and mixed/serous histology (OR = 2.899, 95% CI: 1.933-4.349, P < 0.001).

Table 1. Clinicopathological characteristics according to NDRG1 expression group in the TCGA-UCEC tumor cohort.

Characteristics	NDRG1-low	NDRG1-high	P value
n	**277**	**277**	
Clinical stage, n (%)			**0.061**
Stage I	187 (67.5%)	156 (56.3%)	
Stage II	22 (7.9%)	30 (10.8%)	
Stage III	56 (20.2%)	74 (26.7%)	
Stage IV	12 (4.3%)	17 (6.1%)	
Primary therapy outcome, n (%)			**0.332**
PD	6 (2.5%)	14 (5.8%)	
CR	227 (93.8%)	217 (90.4%)	
SD	3 (1.2%)	3 (1.2%)	

Characteristics	NDRG1-low	NDRG1-high	P value
PR	6 (2.5%)	6 (2.5%)	
Radiation therapy, n (%)			**< 0.001**
Yes	101 (38.3%)	147 (55.5%)	
No	163 (61.7%)	118 (44.5%)	
Diabetes, n (%)			**0.680**
Yes	63 (28.3%)	61 (26.5%)	
No	160 (71.7%)	169 (73.5%)	
Menopause status, n (%)			**0.138**
Pre	23 (9.2%)	12 (4.7%)	
Peri	8 (3.2%)	9 (3.5%)	
Post	220 (87.6%)	235 (91.8%)	
Hormones therapy, n (%)			**0.339**
Yes	26 (15.4%)	21 (11.9%)	
No	143 (84.6%)	156 (88.1%)	
Tumor invasion(%), n (%)			**0.174**
< 50	145 (57.8%)	116 (51.6%)	
>= 50	106 (42.2%)	109 (48.4%)	
Histologic grade, n (%)			**< 0.001**
G1	74 (27.1%)	25 (9.3%)	
G2	72 (26.4%)	49 (18.1%)	
G3	127 (46.5%)	196 (72.6%)	
Histological type, n (%)			**< 0.001**
Endometrioid	233 (84.1%)	179 (64.6%)	
Mixed	7 (2.5%)	17 (6.1%)	
Serous	37 (13.4%)	81 (29.2%)	
Residual tumor, n (%)			**0.265**
R0	196 (92.5%)	181 (89.2%)	
R1	11 (5.2%)	11 (5.4%)	

Characteristics	NDRG1-low	NDRG1-high	P value
R2	5 (2.4%)	11 (5.4%)	
BMI, n (%)			**0.024**
<= 30	94 (35.9%)	118 (45.6%)	
> 30	168 (64.1%)	141 (54.4%)	
Height, n (%)			**0.906**
<= 160	124 (46.8%)	123 (47.3%)	
> 160	141 (53.2%)	137 (52.7%)	
Weight, n (%)			**0.002**
<= 80	104 (39.2%)	139 (52.5%)	
> 80	161 (60.8%)	126 (47.5%)	
Age, n (%)			**0.198**
<= 60	111 (40.2%)	96 (34.9%)	
> 60	165 (59.8%)	179 (65.1%)	
Race, n (%)			**0.038**
Asian	14 (5.4%)	6 (2.4%)	
Black or African American	46 (17.8%)	63 (25.2%)	
White	199 (76.8%)	181 (72.4%)	
OS event, n (%)			**0.042**
Alive	239 (86.3%)	221 (79.8%)	
Dead	38 (13.7%)	56 (20.2%)	
DSS event, n (%)			**0.025**
Yes	23 (8.4%)	40 (14.4%)	
No	252 (91.6%)	237 (85.6%)	
PFI event, n (%)			**0.087**
Yes	56 (20.2%)	73 (26.4%)	
No	221 (79.8%)	204 (73.6%)	

Abbreviations: PD, progressive disease; SD, stable disease; PR, partial response; CR, complete response; OS, overall survival; DSS, disease-specific survival; PFI, progression-free interval. Percentages were calculated from non-missing values within each group.

Fig 3. Associations between NDRG1 expression and clinicopathological characteristics in UCEC. Box plots show NDRG1 expression across pathological stage, histologic grade, and histological type in tumor samples with available annotations. Panel D summarizes independently reconstructed univariate odds ratios from collapsed 2 × 2 contingency tables using NDRG1 group (high vs low) as predictor. Reconstruction details are provided in S5 Text.

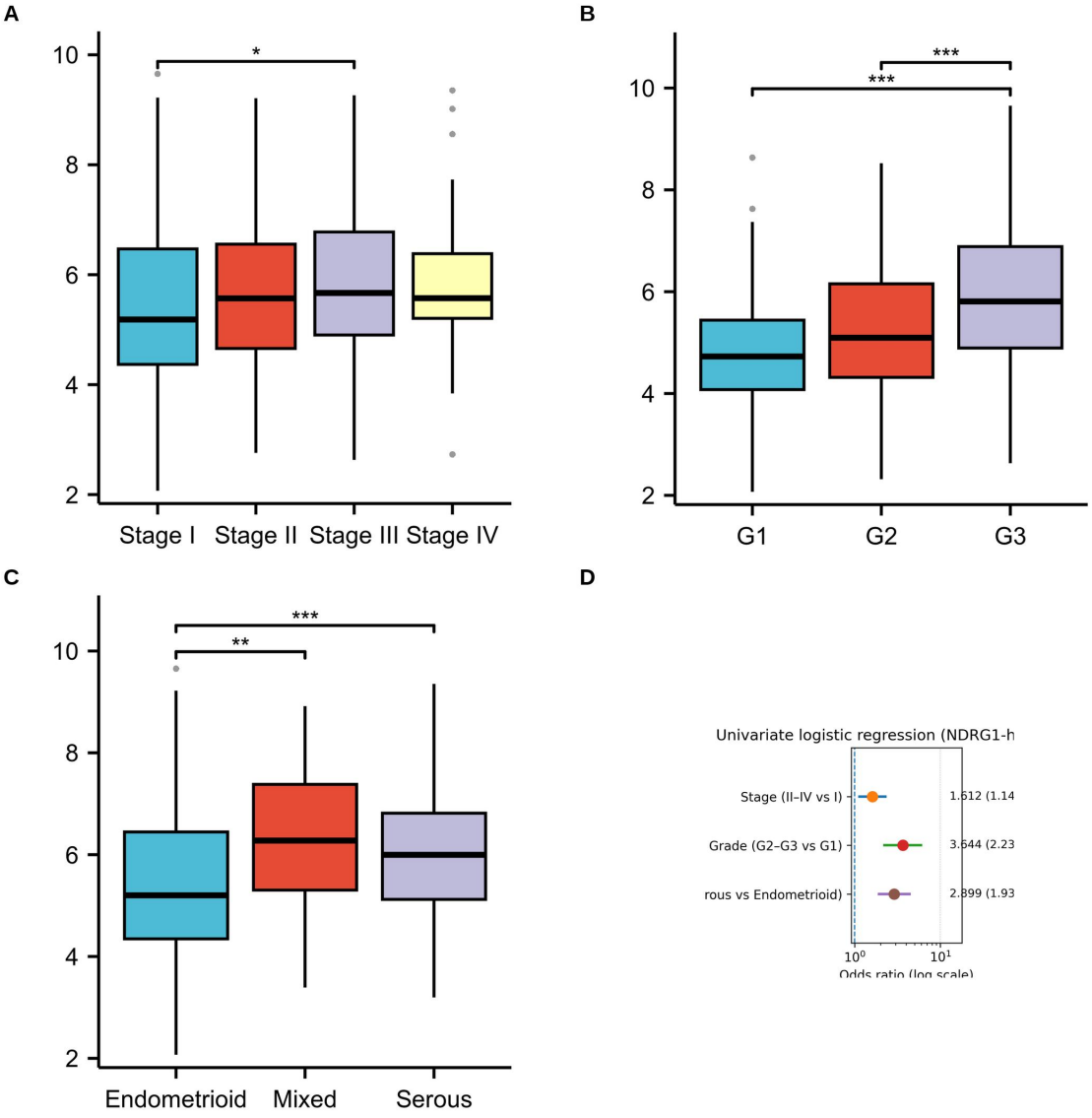

Exploratory TP53-context analyses provide limited support for a direct NDRG1-TP53 link

NDRG1 showed only a weak, non-significant correlation with TP53 mRNA expression in the full TPM cohort (rho = 0.072, P = 0.090). In the matched normalized-expression subset, NDRG1 tended to be higher in TP53-mutant tumors than in TP53-wild-type tumors, but the difference did not reach statistical significance (P = 0.093). TP53-stratified survival sensitivity analyses based on extreme within-stratum NDRG1 quantiles suggested directional heterogeneity, although none of the subgroup comparisons was significant and subgroup event counts were limited.

Time-dependent ROC comparisons of NDRG1 mRNA and TP53 mRNA in the overall cohort yielded only modest AUCs at 1, 3, and 5 years for OS and PFI. NDRG1 outperformed TP53 in several comparisons, but absolute discrimination remained limited. These ROC curves are therefore best interpreted as descriptive performance displays rather than evidence of substantial prognostic utility.

Fig 4. Exploratory TP53-context analyses of NDRG1 in UCEC. (A) Correlation between NDRG1 and TP53 mRNA expression in the full TPM cohort (rho = 0.072, P = 0.090). (B) Comparison of NDRG1 expression by TP53 mutation status in the matched normalized-expression subset (P = 0.093). (C-F) Extreme-quantile sensitivity analyses of OS and PFI within TP53-mutant and TP53-wild-type strata. (G-L) Time-dependent ROC comparisons between NDRG1 mRNA and TP53 mRNA. These panels do not establish a direct TP53-dependent mechanism.

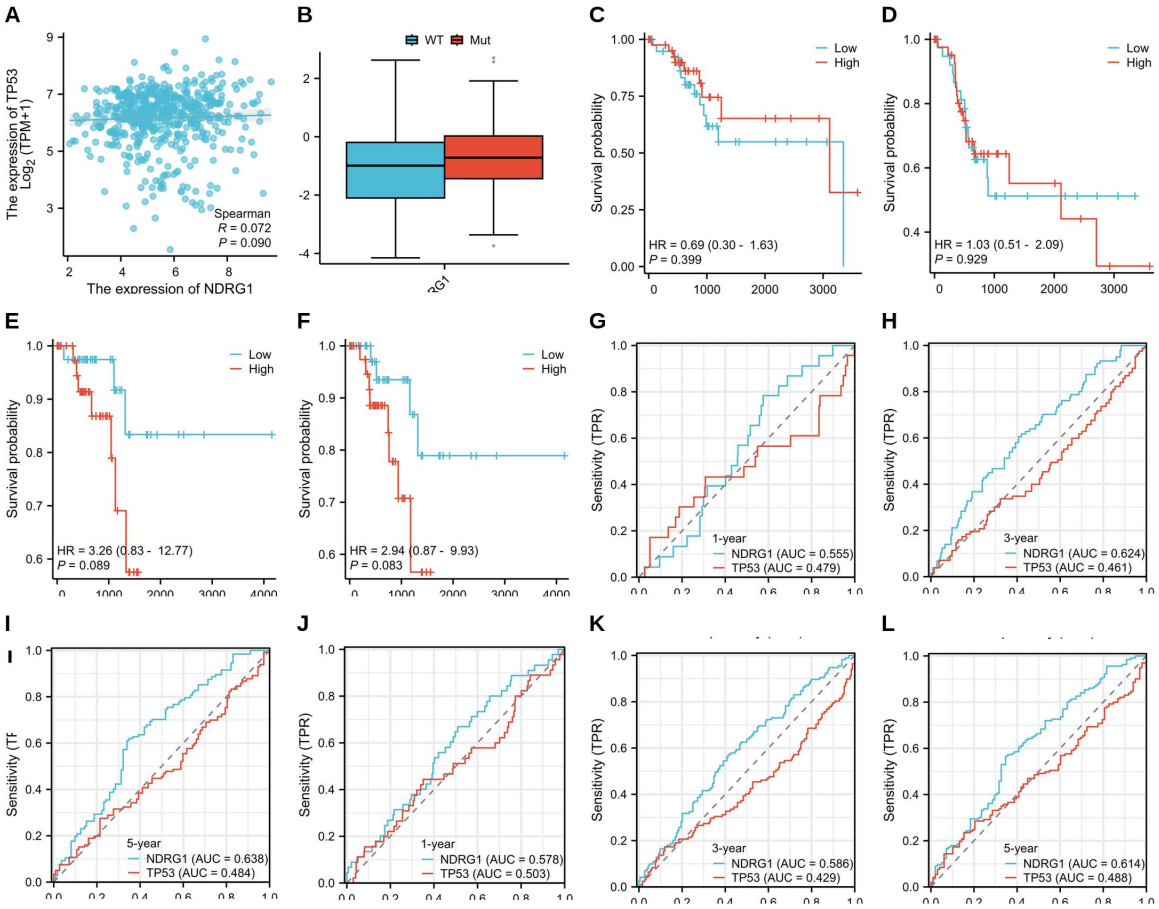

NDRG1 correlates with ferroptosis-related and immune-regulatory genes in a normalized expression cohort

In the normalized HiSeqV2 cohort, NDRG1 was positively correlated with multiple ferroptosis-related genes, including ATG5 (rho = 0.286, P = 0.0001), TFRC (rho = 0.258, P = 0.0005), and FTH1 (rho = 0.272, P = 0.000263). NDRG1 also correlated positively with VTCN1 (rho = 0.368, P = 4.98×10^-7) and inversely with CTLA4 (rho = -0.229, P = 0.0023). Although modest in magnitude, these associations were reproducible across the heatmaps and representative scatter plots, and several NDRG1-centric correlations remained significant after Benjamini-Hochberg correction.

Fig 5. Correlations of NDRG1 with ferroptosis-related and immune-regulatory genes in a normalized TCGA-UCEC cohort. Heatmaps show Spearman correlation structure for selected ferroptosis regulators/markers and immune checkpoint or immunoregulatory genes (n = 176). Representative scatter plots show correlations with ATG5, TFRC, VTCN1, and CTLA4. Benjamini-Hochberg-adjusted summaries are provided in the supporting files where indicated.

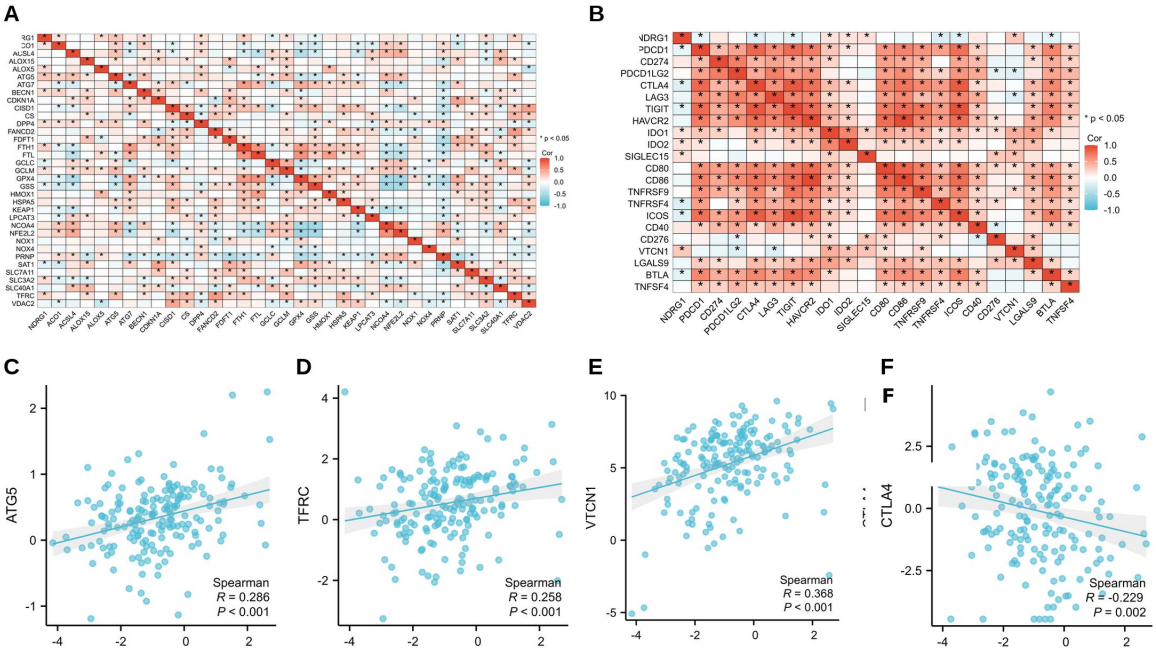

Ferroptosis-score patterns are more evident across TP53-defined subgroups than in global correlation analyses

In the mutation-annotated subset (n = 168), FerroptosisScore differed significantly between TP53-wild-type and TP53-mutant tumors (P = 3.46×10^-4) and across the four TP53×NDRG1 subgroups defined by TP53 status and median NDRG1 expression (P = 0.00159). By contrast, the continuous association between NDRG1 and FerroptosisScore remained weak in the broader normalized cohort available for this comparison.

Taken together, the signal in Fig 6 is more consistent with subgroup-level structure than with a strong global linear relationship. Because panels A-B and panel C were derived from related but non-identical analytic subsets, they should be interpreted as complementary exploratory views rather than as a single internally uniform inferential chain.

Fig 6. Exploratory ferroptosis-score analyses across TP53 and NDRG1 strata in UCEC. A ferroptosis activity score (FerroptosisScore) was derived by ssGSEA/GSVA using a curated ferroptosis regulator set. (A) Comparison between TP53-wild-type and TP53-mutant tumors in the mutation-annotated subset (WT n = 79, Mut n = 89). (B) Comparison across four TP53 × NDRG1 subgroups in the same subset. (C) Continuous correlation between NDRG1 and FerroptosisScore in the broader normalized cohort used for this panel. (D) Descriptive subgroup-summary display of representative ferroptosis-related features. Because panels A-B and C were derived from different analytic subsets, this figure should be interpreted cautiously.

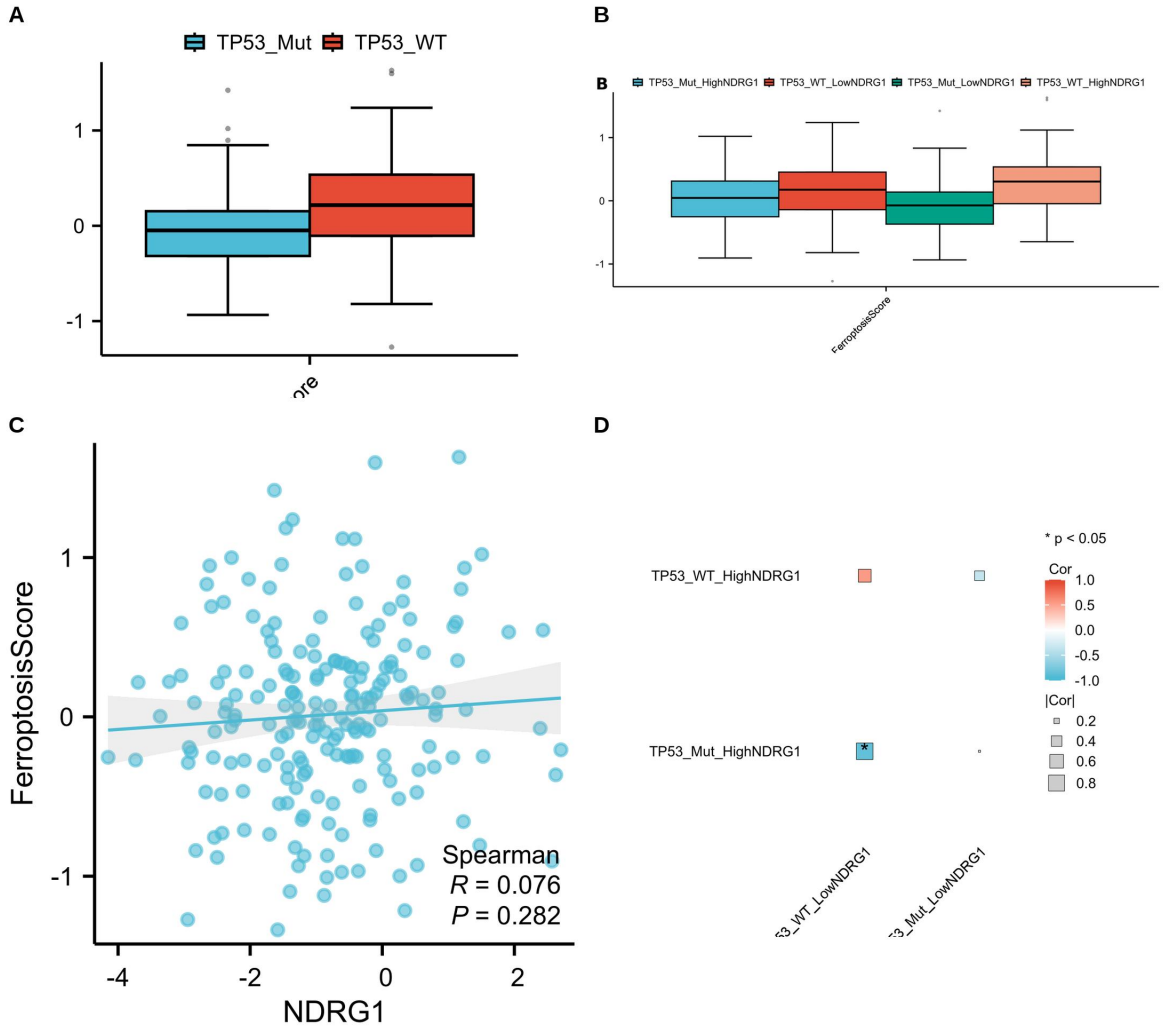

GSEA links NDRG1-high tumors to p53-related and epithelial differentiation programs, with weaker support for ferroptosis

GSEA of genes ranked by differential expression between NDRG1-low and NDRG1-high tumors showed strong enrichment of epithelial differentiation and cornification-related pathways in NDRG1-high tumors. Among biologically targeted pathways, a p53 downstream pathway was clearly enriched in NDRG1-high tumors (NES = -1.565, FDR = 0.015). A ferroptosis pathway also trended toward enrichment in NDRG1-high tumors, although the signal was weaker (NES = -1.555, FDR = 0.096) and is best regarded as suggestive rather than definitive.

Fig 7. Gene set enrichment analysis (GSEA) of NDRG1-associated pathways in UCEC. Genes were ranked by differential expression between NDRG1-low and NDRG1-high tumors and analyzed against MSigDB canonical pathways. Negative normalized enrichment scores indicate enrichment in NDRG1-high tumors. The p53 downstream pathway showed stronger support, whereas ferroptosis-related enrichment was suggestive rather than definitive.

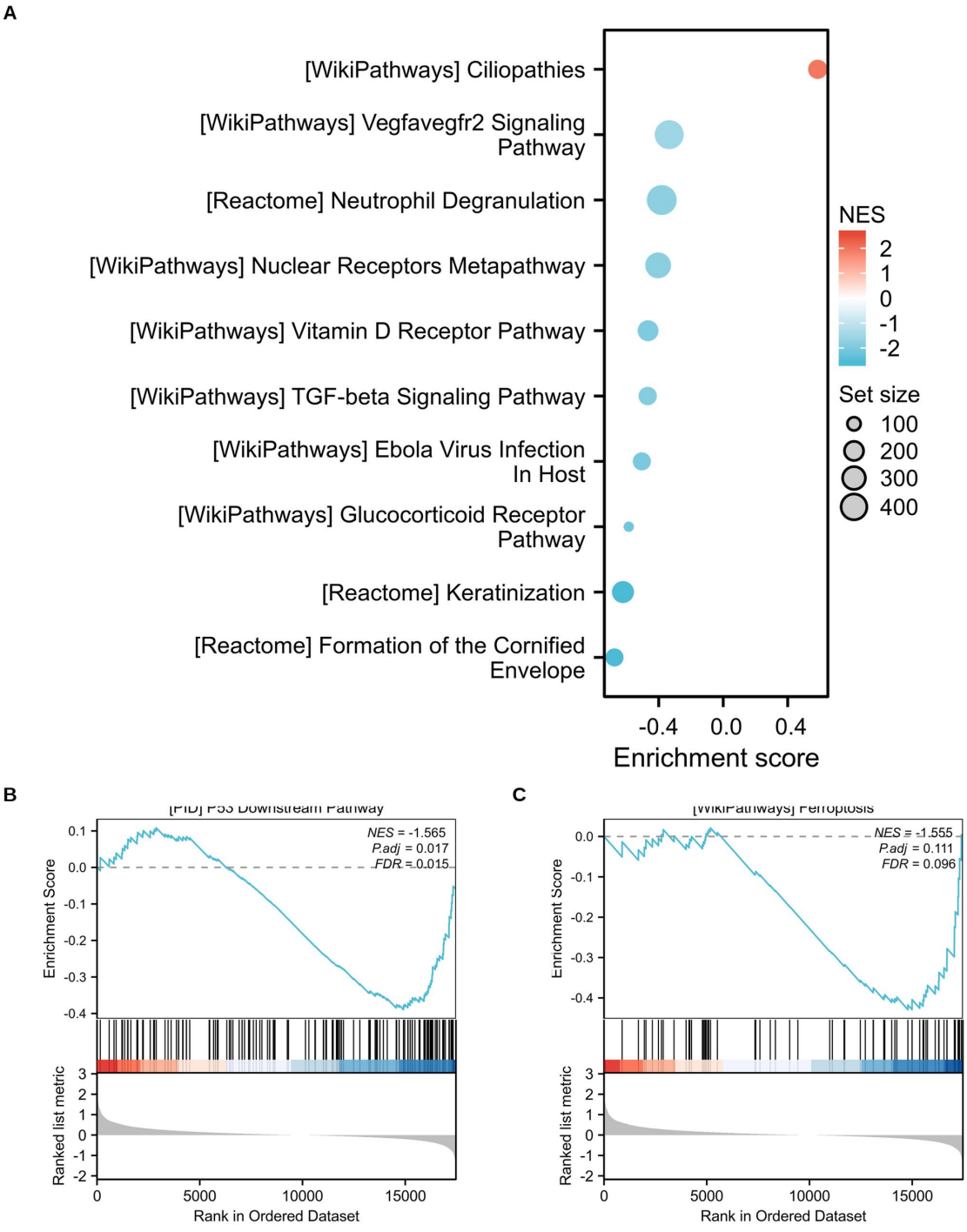

An exploratory complete-case PFI model provides limited internal discrimination

In the complete-case cohort used for exploratory modeling, none of the candidate clinical or molecular variables remained independently significant in the multivariable Cox model. The resulting nomogram

and related diagnostics therefore describe the behavior of a weak internal model rather than a validated prediction tool.

These analyses did not support clinical application of the model. Instead, Fig 8 shows that age, stage, grade, TP53 mutation status, NDRG1, and FerroptosisScore, as assembled here, yielded limited internal discrimination in a relatively small complete-case subset (C-index = 0.576, 95% CI: 0.536-0.616). External validation and model redevelopment would be required before any prognostic use could be considered.

Fig 8. Internal diagnostics of an exploratory PFI model in UCEC. (A) Multivariable Cox regression in the complete-case cohort (n = 165). (B-I) Nomogram, calibration, decision-curve, and time-dependent ROC displays generated for internal model appraisal only. Because no covariate was independently significant and discrimination was limited, these panels should not be interpreted as evidence of clinical utility.

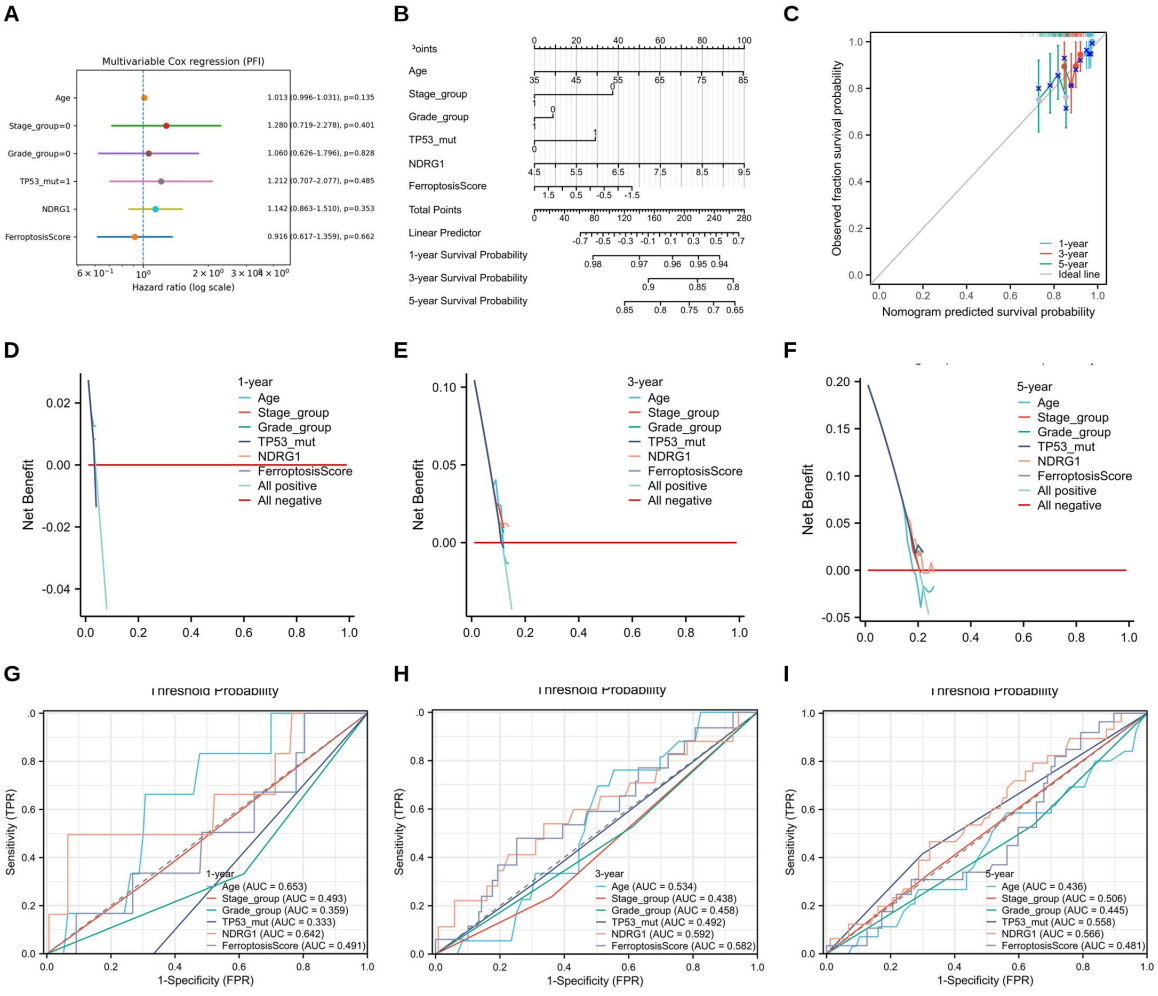

Discussion

This study provides an integrated analysis of public UCEC data spanning differential expression, prognosis, clinicopathological associations, TP53-context analyses, ferroptosis-related correlations, pathway enrichment, and exploratory prognostic modeling. The most robust findings were the tumor-normal expression comparisons, survival associations in the full TPM cohort, clinicopathological

correlations, and normalized-cohort associations linking NDRG1 with ferroptosis-related and immune-regulatory genes.

NDRG1 was lower in UCEC tumors than in normal endometrium, yet higher intratumoral NDRG1 expression identified patients with worse outcome. This apparent paradox is biologically plausible because downregulation relative to normal tissue and adverse stratification within tumors are not mutually exclusive. A recent study of endometrioid endometrial carcinoma likewise associated high NDRG1 expression with poor prognosis[23].

The TP53-related findings should still be interpreted cautiously. The full-cohort correlation between NDRG1 and TP53 mRNA was weak, and the mutation-stratified expression difference amounted only to a trend. Although TP53-stratified extreme-quantile survival curves suggested that the direction of association might vary by TP53 status, these analyses excluded the middle 60% of samples and were constrained by small event counts. The biological and clinical complexity of p53-abnormal endometrial tumors supports such caution[24].

The ferroptosis-related findings were mixed but informative. A recent endometrial cancer review emphasized that ferroptosis in this disease is strongly context dependent[25], and a broader oncology synthesis reached a similar conclusion across tumor types[26]. The inverse association with selected immune-checkpoint features should likewise be interpreted cautiously, but emerging evidence indicates that antitumor immunity can intersect with tumor-cell ferroptosis[27]. The positive correlations with ATG5 and TFRC are biologically plausible because autophagy-mediated ferritin turnover can promote ferroptosis[28], and TFRC has been proposed as a ferroptosis marker[29]. Experimental work in hepatocellular carcinoma further suggests that NDRG1 can modulate ferroptosis in another tumor context, although whether that observation generalizes to UCEC remains unknown[30].

The exploratory prognostic model should be viewed strictly as an internal demonstration. None of the covariates was independently significant, the C-index was low, and the calibration, DCA, and ROC displays did not justify clinical adoption.

Several limitations deserve emphasis. First, this was a retrospective bioinformatics study without external validation or functional experimentation. Second, different public-data subsets and expression scales were necessarily used across analyses because the available normalized matrices and matched TP53 annotations did not cover every sample in the full TPM cohort. Third, some panels, particularly the TP53-stratified extreme-quantile analyses and the complete-case predictive model, were exploratory by design.

Overall, the present results suggest that NDRG1 marks an adverse clinicopathological and prognostic phenotype in UCEC and resides within a broader transcriptional context involving p53-related stress programs, immune-regulatory states, and ferroptosis-linked genes. These findings support NDRG1 as a candidate biomarker for molecular stratification and as a plausible entry point for future mechanistic studies of TP53-ferroptosis crosstalk in UCEC.

Conclusions

NDRG1 is dysregulated in UCEC and, within tumors, higher expression is associated with aggressive clinicopathological features and poorer survival. Public-data analyses further place

NDRG1 within a TP53-related transcriptional context linked to ferroptosis-associated genes and immunoregulatory checkpoints, with pathway analysis supporting enrichment of p53 downstream signaling in NDRG1-high tumors. Together, these findings nominate NDRG1 as a candidate biomarker for prognostic and biological stratification and as a potential entry point for mechanistic studies of TP53-ferroptosis crosstalk in UCEC.

Abbreviations

UCEC, uterine corpus endometrial carcinoma; NDRG1, N-myc downstream-regulated gene 1; OS, overall survival; DSS, disease-specific survival; PFI, progression-free interval; ssGSEA, single-sample gene set enrichment analysis; GSEA, gene set enrichment analysis; TPM, transcripts per million; HR, hazard ratio; CI, confidence interval; OR, odds ratio; DCA, decision curve analysis.

Data availability

All public-source data used in this study are accessible without special privileges. TCGA-UCEC RNA-seq expression, clinical annotations, and mutation-linked identifiers were obtained from publicly accessible TCGA/GDC-derived resources and harmonized by sample identifier where required. Survival endpoints were obtained from the TCGA Pan-Cancer Clinical Data Resource (TCGA-CDR). Selected mutation-stratified and normalized-matrix analyses were generated from public expression tables after sample-ID matching; panel-specific cohort definitions are summarized in S5 Text.

Ethics statement

Not applicable. This study used publicly available de-identified datasets and did not involve new recruitment of human participants or new animal experiments.

Competing interests

The authors declare that they have no competing interests.

Funding

This work was supported by the Inner Mongolia Natural Science Foundation (2024MS08024) and the Inner Mongolia Public Hospital Joint Scientific Research Project (2023GLLH0091).

Authors' contributions

Y.Y. and J.M. conceived and designed the study. Y.Y. performed data acquisition, data processing, bioinformatics analyses, and manuscript drafting. Y.Z., Y.Q., BY., and H.C.assisted with data curation, figure review, and manuscript revision. J.M. supervised the study and approved the final manuscript. All authors read and approved the final manuscript.

Acknowledgments

We acknowledge TCGA, the Genomic Data Commons, and the TCGA-CDR resource for making the public data used in this study available.

References

1. Bray F, Laversanne M, Sung H, Ferlay J, Siegel RL, Soerjomataram I, et al. Global cancer statistics 2022: GLOBOCAN estimates of incidence and mortality worldwide for 36 cancers in 185 countries. CA Cancer J Clin. 2024;74(3):229-263. doi:10.3322/caac.21834.
2. Makker V, MacKay H, Ray-Coquard I, Levine DA, Westin SN, Aoki D, et al. Endometrial cancer. Nat Rev Dis Primers. 2021;7(1):88. doi:10.1038/s41572-021-00324-8.
3. Cancer Genome Atlas Research Network, Kandoth C, Schultz N, Cherniack AD, Akbani R, Liu Y, et al. Integrated genomic characterization of endometrial carcinoma. Nature. 2013;497(7447):67-73. doi:10.1038/nature12113.
4. Dixon SJ, Lemberg KM, Lamprecht MR, Skouta R, Zaitsev EM, Gleason CE, et al. Ferroptosis: an iron-dependent form of nonapoptotic cell death. Cell. 2012;149(5):1060-1072. doi:10.1016/j.cell.2012.03.042.
5. Stockwell BR, Friedmann Angeli JP, Bayir H, Bush AI, Conrad M, Dixon SJ, et al. Ferroptosis: a regulated cell death nexus linking metabolism, redox biology, and disease. Cell. 2017;171(2):273-285. doi:10.1016/j.cell.2017.09.021.
6. Jiang X, Stockwell BR, Conrad M. Ferroptosis: mechanisms, biology and role in disease. Nat Rev Mol Cell Biol. 2021;22(4):266-282. doi:10.1038/s41580-020-00324-8.
7. Lei G, Zhuang L, Gan B. Targeting ferroptosis as a vulnerability in cancer. Nat Rev Cancer. 2022;22(7):381-396. doi:10.1038/s41568-022-00459-0.
8. Jiang L, Kon N, Li T, Wang SJ, Su T, Hibshoosh H, et al. Ferroptosis as a p53-mediated activity during tumour suppression. Nature. 2015;520(7545):57-62. doi:10.1038/nature14344.
9. Liu Y, Gu W. p53 in ferroptosis regulation: the new weapon for the old guardian. Cell Death Differ. 2022;29(5):895-910. doi:10.1038/s41418-022-00943-y.
10. Ellen TP, Ke Q, Zhang P, Costa M. NDRG1, a growth and cancer related gene: regulation of gene expression and function in normal and disease states. Carcinogenesis. 2008;29(1):2-8. doi:10.1093/carcin/bgm200.
11. Kovacevic Z, Richardson DR. The metastasis suppressor, Ndrg-1: a new ally in the fight against cancer. Carcinogenesis. 2006;27(12):2355-2366. doi:10.1093/carcin/bgl146.
12. Joshi V, Lakhani SR, McCart Reed AE. NDRG1 in cancer: a suppressor, promoter, or both? Cancers (Basel). 2022;14(23):5739. doi:10.3390/cancers14235739.
13. Chen J, Li S, Yang Z, Lu G, Hu H. Correlation between NDRG1 and PTEN expression in endometrial carcinoma. Cancer Sci. 2008;99(4):706-710. doi:10.1111/j.1349-7006.2008.00749.x.
14. Croessmann S, Wong HY, Zabransky DJ, Chu D, Mendonca J, Sharma A, et al. NDRG1 links p53 with proliferation-mediated centrosome homeostasis and genome stability. Proc Natl Acad Sci U S A. 2015;112(37):11583-11588. doi:10.1073/pnas.1503683112.
15. Liu J, Lichtenberg T, Hoadley KA, Poisson LM, Lazar AJ, Cherniack AD, et al. An integrated TCGA pan-cancer clinical data resource to drive high-quality survival outcome analytics. Cell. 2018;173(2):400-416.e11. doi:10.1016/j.cell.2018.02.052.
16. Zhou N, Bao J. FerrDb: a manually curated resource for regulators and markers of ferroptosis and ferroptosis-disease associations. Database (Oxford). 2020;2020:baaa021. doi:10.1093/database/baaa021.
17. Hänzelmann S, Castelo R, Guinney J. GSVA: gene set variation analysis for microarray and RNA-seq data. BMC Bioinformatics. 2013;14:7. doi:10.1186/1471-2105-14-7.

18. Subramanian A, Tamayo P, Mootha VK, Mukherjee S, Ebert BL, Gillette MA, et al. Gene set enrichment analysis: a knowledge-based approach for interpreting genome-wide expression profiles. Proc Natl Acad Sci U S A. 2005;102(43):15545-15550. doi:10.1073/pnas.0506580102.
19. Iasonos A, Schrag D, Raj GV, Panageas KS. How to build and interpret a nomogram for cancer prognosis. J Clin Oncol. 2008;26(8):1364-1370. doi:10.1200/JCO.2007.12.9791.
20. Collins GS, Reitsma JB, Altman DG, Moons KGM. Transparent reporting of a multivariable prediction model for individual prognosis or diagnosis (TRIPOD): the TRIPOD statement. Ann Intern Med. 2015;162(1):55-63. doi:10.7326/M14-0697.
21. Blanche P, Dartigues JF, Jacqmin-Gadda H. Estimating and comparing time-dependent areas under receiver operating characteristic curves for censored event times with competing risks. Stat Med. 2013;32(30):5381-5397. doi:10.1002/sim.5958.
22. Vickers AJ, Elkin EB. Decision curve analysis: a novel method for evaluating prediction models. Med Decis Making. 2006;26(6):565-574. doi:10.1177/0272989X06295361.
23. Ijichi M, Ushijima K, Yamaguchi T, Nishida N, Tasaki K, Park J, et al. High expression of NDRG1 is a poor prognostic factor in patients with endometrial endometrioid carcinoma with long-term observation. Kurume Med J. 2025;71(1-2):11-18. doi:10.2739/kurumemedj.MS7112004.
24. Casanova J, Babiciu A, Duarte GS, da Costa AG, Serra SS, Costa T, et al. Abnormal p53 high-grade endometrioid endometrial cancer: a systematic review and meta-analysis. Cancers (Basel). 2025;17(1):38. doi:10.3390/cancers17010038.
25. Žalytė E. Ferroptosis, metabolic rewiring, and endometrial cancer. Int J Mol Sci. 2024;25(1):75. doi:10.3390/ijms25010075.
26. Zhou Q, Meng Y, Li D, Yao L, Le J, Liu Y, et al. Ferroptosis in cancer: from molecular mechanisms to therapeutic strategies. Signal Transduct Target Ther. 2024;9(1):55. doi:10.1038/s41392-024-01769-5.
27. Wang W, Green M, Choi JE, Gijon M, Kennedy PD, Johnson JK, et al. CD8+ T cells regulate tumour ferroptosis during cancer immunotherapy. Nature. 2019;569(7755):270-274. doi:10.1038/s41586-019-1170-y.
28. Hou W, Xie Y, Song X, Sun X, Lotze MT, Zeh HJ 3rd, et al. Autophagy promotes ferroptosis by degradation of ferritin. Autophagy. 2016;12(8):1425-1428. doi:10.1080/15548627.2016.1187366.
29. Feng H, Schorpp K, Jin J, Yozwiak CE, Hoffstrom BG, Decker AM, et al. Transferrin receptor is a specific ferroptosis marker. Cell Rep. 2020;30(10):3411-3423.e7. doi:10.1016/j.celrep.2020.02.049.
30. Li L, Wu T, Gong G, Li B, Feng J, Xu L, et al. NDRG1 alleviates Erastin-induced ferroptosis of hepatocellular carcinoma. BMC Cancer. 2025;25(1):522. doi:10.1186/s12885-025-13954-y.

Supporting information captions

S1 Dataset. Complete-case cohort (n=165) used for exploratory PFI modeling.

S2 Table. Multivariable Cox output for the exploratory PFI model.

S3 Dataset. Model-derived risk scores for the exploratory complete-case cohort.

S4 Table. Full GSEA results for the ranked NDRG1-low versus NDRG1-high comparison.

S5 Text. Figure-to-dataset/sample-size mapping, manual reconstruction details for Fig 3D, and provenance notes for final Fig 6-Fig 8.

S6 File. Source bundle containing the raw CSV/XLSX tables and original public-data export tables used to trace final Fig 6-Fig 8.